Research Report
TRIUMF Student Program
Summer 2015

Peter Collins

September 10, 2015

Abstract

This report contains the experiments and projects undertaken while working at TRIUMF during the summer of 2015. They were as follows:

1. The structure of the magnetic field inside of the H- ion sources used in the cyclotron at TRIUMF is largely unknown. A rotating coil device was constructed to map the multi-pole structure magnetic field of these sources and it was tested using a Helmholtz coil.

2. The lifetime of the filaments used in the main ion source of TRIUMF (I1) has recently worsened. It is believed that this is due to outside gases leaking into the system. The effects of contaminant gases on filament lifetime were studied using the ion source test bench (I3). A linear dependence between filament lifetime and the partial pressure of a contaminant gas was found.

3. An electrode was installed in the I3 ion source body to study its ability to pulse the extracted beam. Measurements of the beam current subject to low-frequency pulsing and an electrostatic model of the source body were used to determine the electric potential profile inside the source body during pulsing. It was determined from this data that the electrode was unsuitable for high-frequency pulsing of the beam due to unpredictable behaviour of the H- plasma inside the source body.

4. The position of the beam inside the injection line of the cyclotron was seen to exhibit low-frequency oscillations about its design trajectory. A Fourier analysis of the signal from a beam-position monitor on the injection line found that the vacuum pumps on the beam-line were the source of the disturbance. The analysis also revealed high-frequency periodic disturbances in beam-position that were previously unseen.

1 Rotating Coil Device for Magnetic Measurement of H- Ion Source Bodies

1.1 Purpose

A rotating coil device was constructed to perform measurements of the magnetic field inside the multi-cusp volume H- ion sources used in the cyclotron at TRIUMF.

1.2 Introduction to H- Ion Sources

The ion sources used to supply H- ions to the cyclotron at TRIUMF produce hydrogen ions using a process called volume production. This process [**1**] begins with pumping hydrogen gas into the evacuated volume inside the source body. High energy (> 5eV) electrons emitted from a filament collide with the hydrogen molecules to bring them into a high vibrational state. When these excited molecules collide with low energy electrons (≤ 1eV), they split into an H atom and an H- ion through dissociative-attachment:

$$e^- + H_2(v'') \rightarrow H + H^-,$$

where $v'' \geq 6$ is the vibrational state of the hydrogen molecule. These ions are then extracted from the source to form a beam.

The H- plasma within the source is contained by a series of permanent magnets placed along the outside of the source body in what is known as a multi-cusp arrangement. In this arrangement, long permanent magnets are placed with alternating polarity at regularly spaced intervals along the outer wall of the source body . The field lines near the walls of the body form magnetic cusps which reflect incoming ions and electrons. There is an additional cusp arrangement of magnets along the backplate of the ion source to further confine the ions.

H- ions are fragile and collisions with the high energy electrons will destroy them before they can be extracted. To avoid this, a magnetic filter is installed near the extraction aperture which prevents the high-energy electrons from entering the region where the H- ions are extracted. The source bodies at TRIUMF use a pair of permanent magnets to form a dipole filter field in a longitudinal plane near the extraction aperture

The optimal placement and strength of the magnetic filter field is currently determined through trial and error. It is of interest to be able to measure the magnetic field inside of a working ion source body to determine what features the field should exhibit. With this information, one could determine whether or not a source body would work without spending time testing its performance in the ion source.

1.3 Theory of Harmonic Coil Measurements

The following section is based on the Magnetic Measurements chapter of the Handbook of Accelerator Physics and Engineering (2013). The magnetic field components along the axis of accelerator magnets, or in this case an ion source body, can be considered to be 2D in the region far from the ends. The field components in cylindrical coordinates can then be written as

$$
\begin{aligned}
B_r(r,\theta) &= \sum_{n=1}^{\infty} C(n) \left(\frac{r}{R_{ref}}\right)^{n-1} \sin[n(\theta-\alpha_n)] \\
B_\theta(r,\theta) &= \sum_{n=1}^{\infty} C(n) \left(\frac{r}{R_{ref}}\right)^{n-1} \cos[n(\theta-\alpha_n)]
\end{aligned}
\tag{1}
$$

where $C(n)$ are the strength of the 2n-pole components of the field and α_n a parameter determining their orientation. R_{ref} is a reference radius and is typically chosen to be 50-70% of the magnet radius.

The coefficients $C(n)$ can be determined by rotating a pickup coil about the magnet axis. To demonstrate this, we examine the case of a tangential coil: consider a rectangular coil with N turns, length L, and width Δ mounted lengthwise on the surface of a cylinder of radius R_C. The flux $\Phi(\theta)$ through the coil at any angular position θ can be calculated from Eq.(1),

$$
\begin{aligned}
\Phi(\theta) &= \sum_{n-1}^{\infty} \frac{P_t}{n} C(n) sin(n\theta - n\alpha_n) \\
\text{where } P_t &= 2NLR_{ref} \left(\frac{R_C}{R_{ref}}\right)^n \sin\left(\frac{n\Delta}{2}\right).
\end{aligned}
\tag{2}
$$

If the coil rotates with angular velocity ω , the voltage induced is

$$
V(t) = -\frac{d\Phi}{dt} = -\sum_{n=1}^{\infty} \omega P_t C(n) \cos(n\omega t + n\delta - n\alpha_n) \tag{3}
$$

where δ is the angular position at $t = 0$. The field coefficients $C(n)$ can be found by a Fourier analysis of $V(t)$.

1.4 Equipment and Software

The rotating coil device that was modified for this project was originally used for performing magnetic measurements of quadrupole and sextupole accelerator magnets. It originally featured two coils: a small coil for measuring point-harmonics and a long coil for measuring integrated harmonics. It was found that the small coil was not sensitive enough to measure the filter field of the source body so it was disconnected and another coil was made. The new coil measures 1.5mm x 3.0mm with 10 turns and it is mounted to the surface of the plexiglass cylinder, its length parallel to the rotation axis. The long integrating coil was left connected in case it was needed for future tests.

Included with the rotating coil was a laptop featuring software that would process the signal from the coils and the shaft encoder. The laptop, however, was obsolete and the software could not be made to work on a modern computer so new methods of retrieving and processing data from the device were developed. The output of the encoder and harmonic coil were connected to a digital oscilloscope that can save and export waveforms. An external power supply was required to power the shaft encoder since it originally received its power from the laptop.

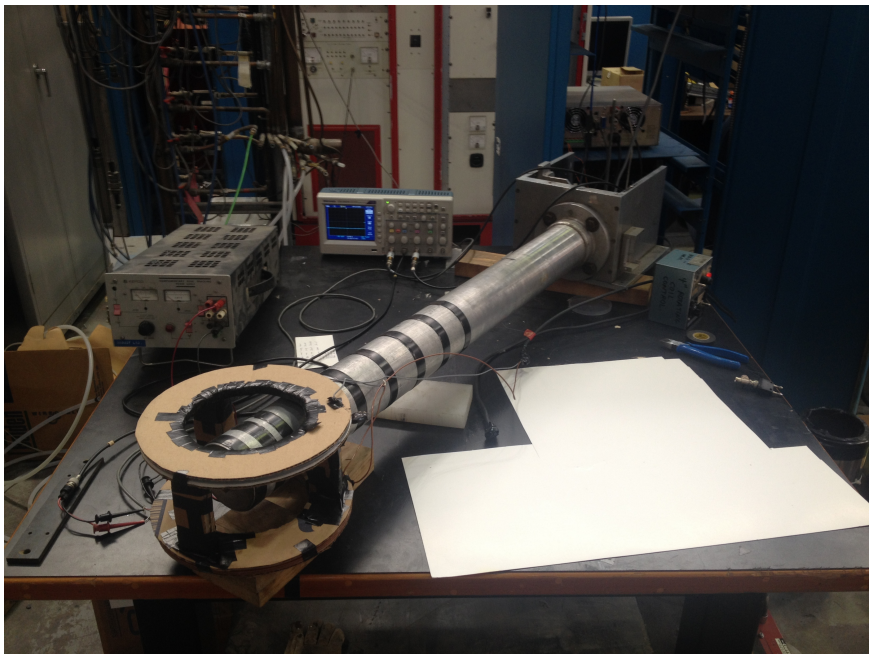

Figure 1: The rotating coil device performing measurements of the Helmholtz coil field

A program to process the waveforms exported from the oscilloscope was written in Python. The program first calculates the rotation frequency of the motor based on the encoder data file and the specifications of the encoder. This calculated rotation frequency is then used to trim the coil waveform such that it contains a whole number of periods. A Fourier transform is performed on the trimmed waveform and the results are plotted and saved.

A Helmholtz coil was constructed to test the harmonic coil. Each coil consists of 18 turns of 14 gauge AWG copper wire wrapped around a cardboard disc of radius 4.5". This coil was operated at 12 amps for this experiment, so, by the well-known Helmholtz coil formula,

$$B = \left(\frac{4}{5}\right)^{3/2} \frac{\mu_0 n I}{R} \approx 17Gs,$$

where B is the magnetic field strength at the center of the Helmholtz coil, n the number of turns, I the current, R the radius, and μ_0 the permeability of free-space.

1.5 Procedure

Measurements of the Helmholtz coil magnetic field were performed following these steps:

- Connected cables:
  - Black and red wires of encoder to variable power supply
  - Black and green wires of encoder to channel 1 of oscilloscope

  - Short coil output to channel 2 of oscilloscope with 20kHz HPF to reduce noise

- Turned on encoder power supply and set to 5V
- Positioned the Helmholtz coil with the small point-harmonic coil located at its center.
- Started the rotating coil. Gradually increased rotation speed to 13Hz ("7" on the dial) and waited for the speed to stabilize.
- Turned on power to the Helmholtz coil
- Adjusted the oscilloscope so that 2-3 periods of the harmonic coil waveform were visible.
- Smoothed waveform using the oscilloscope's averaging function and exported it to the USB drive
- Changed to the encoder's channel and adjusted the oscilloscope so that 8-10 peaks of the encoder waveform were visible
- Exported encoder waveform to the USB drive
- Turned off equipment
- Processed data with computer program

Measurements were performed quickly as the mechanical components of the rotating coil have a limited lifetime. Quick measurements also reduced error due to variations in rotation speed between the saving of the two waveforms.

1.6 Results

Figure 2 shows that the rotating coil measured the magnetic field at the center of the Helmholtz coil to be primarily a dipole field with weak higher-order moments. The higher-order moments are most likely due to imperfections in the coil construction and the fact that the rotating coil sweeps through off-axis regions where the magnetic field is not necessarily uniform.

1.7 Discussion

This test demonstrates that the modified rotating coil device is capable of accurately measuring the multi-pole coefficients of an arbitrary 2D magnetic field and therefore can be used to study the magnetic field of the H- ion sources at TRIUMF.

It should be noted that no information about the phase angle of the multi-pole moments is given by the harmonic analysis. This was an oversight and could easily be fixed by adding new code to the existing program.

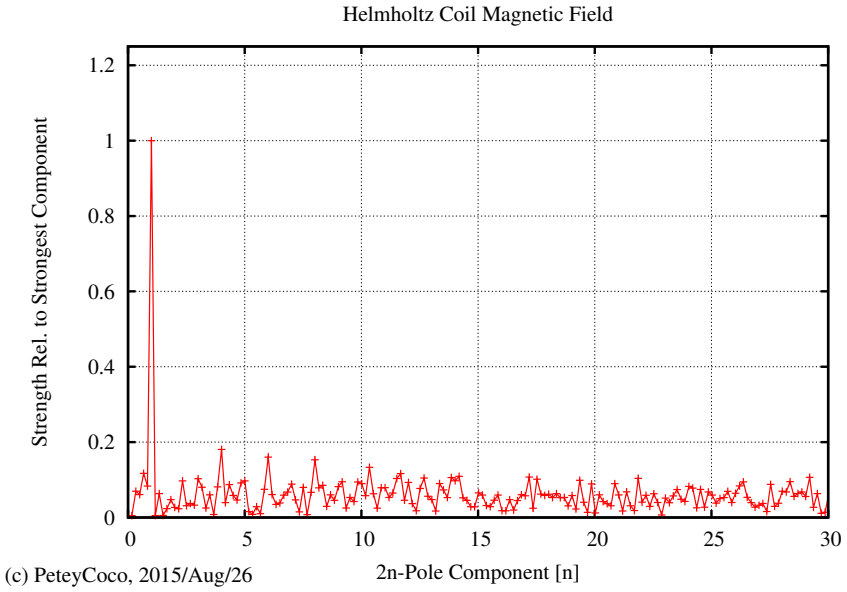

Figure 2: Multi-pole moments of the Helmholtz coil magnetic field

2 Controlled Leak Test

2.1 Purpose

To study how the presence of various species of gases in the H- ion source impacts the lifetime of the filament.

2.2 Equipment

An apparatus was installed for introducing controlled leaks of a gas into the hydrogen fuel line of the source body at the ion source test bench (I3). The gas was stored in a small canister at a pressure of 10-30 psi and a high-precision hand-valve is used to control the amount of gas leaking into the system. A residual gas analyser (RGA) was installed downstream of the ion source to measure the partial pressures of various species in the vacuum.

An EPICS interface allows the user to adjust and monitor all system parameters of I3.

2.3 Method

Tests were performed using nitrogen, helium, argon, and neon gas. The EPICS strip tool was used to record the filament current, vacuum pressure, arc current, arc voltage and hydrogen flow during the experiment. Once a gas was transferred into the canister and a baseline filament current decay rate was established, a leak could be introduced into the system. The following procedure was used for each leak:

- Turned off the filament to stop the arc current

- Opened the cage containing the ion source and the leak apparatus
- Recorded the partial pressures from RGA
- Opened the hand-valve until the desired pressure was observed on the RGA
- Recorded the partial pressures from RGA
- Closed the cage
- Turned on filament and arc
- Set PID loop to maintain 7.0A of arc current at 100V of arc voltage
- Waited for the rate of filament current loss to stabilize
- Calculate the rate of filament current loss from the EPICS data

The time that the source was off needed to be minimized, otherwise it would take longer for the rate of filament current loss to stabilize.

2.4 Results

In Figure 3, the current slope is plotted against the partial pressure of the gas and a linear fit curve is applied to the data. The EPICS data from the series of neon and argon leaks are plotted in Figure 4. The slope for each leak was calculated from portions of the filament current curve that had an approximately constant slope.

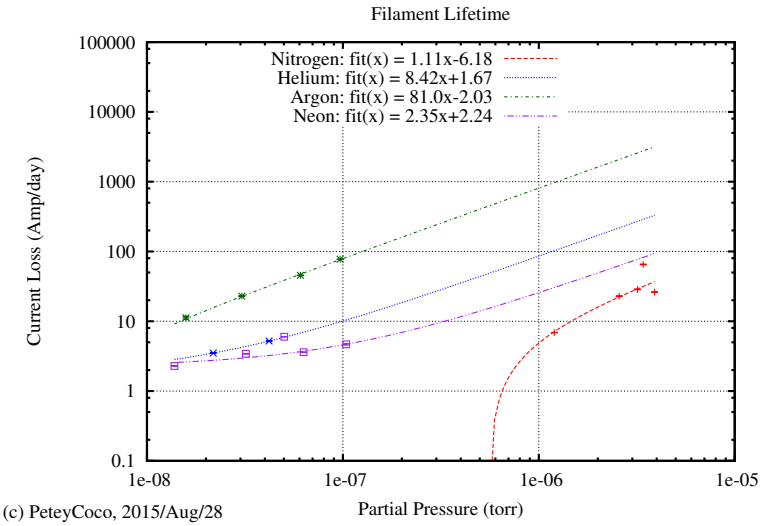

Figure 3: Current loss for each set of leaks and their linear fit curves. The units of the fit curves are in Amp/day with the slopes in Amp/(day · torr). Data for nitrogen is unreliable due to being measured before the current experimental procedure had been developed.

2.5 Discussion

The linear fit curves in Figure 3 are seen to match the data quite well, demonstrating that the current loss in the filament is proportional to the partial pressure of a species of gas present in the ion source body (For reference, the rate of current loss under normal operation is between 2-5 Amp/day). The dependence of the filament current loss on properties of the gases, (i.e. mass, size, etc), is to be studied in future experiments.

It can be seen why it was important to let the current slope stabilize before taking measurements from Figure 4a: when the partial pressure of neon was increased, the filament current would experience a steep drop which would then stabilize after several hours. Conversely, when the partial pressure was decreased, the filament current would increase rapidly for several hours before it returned to a steady downward slope. Similar behaviour was seen with all gases, however the effect was less noticeable when a gas would cause a steep filament current decay slope (see argon in Figure 4b). Due to the symmetric nature of this phenomena, it is hypothesized that the filament undergoes some reversible change when the partial pressures of a gas is increased or decreased. The tests involving nitrogen and helium were performed before this behaviour was noticed. At the time of this writing, new tests with helium gas were in progress and tests with nitrogen were to follow.

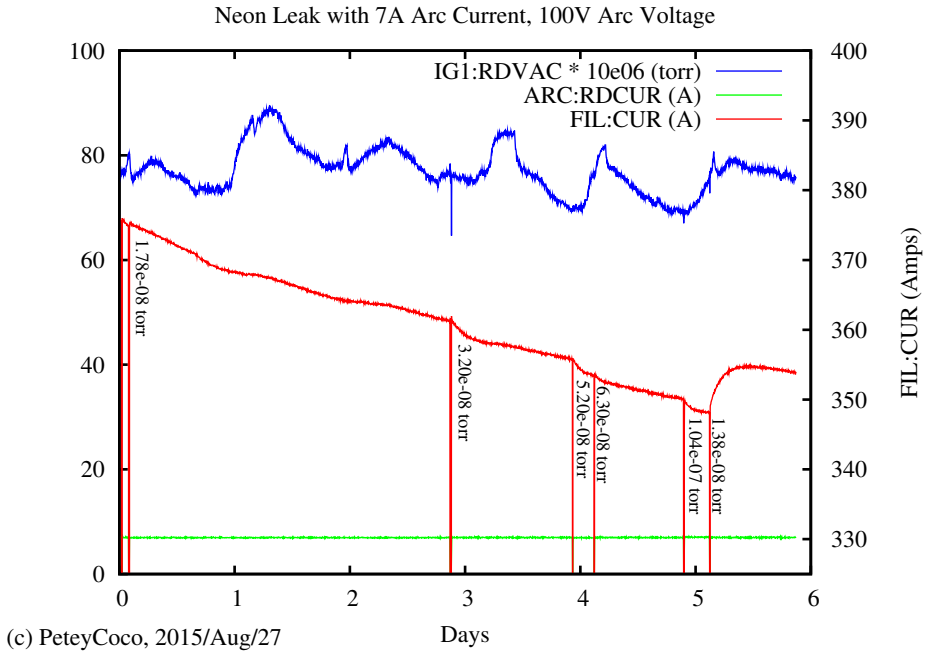

(a) Neon Leak

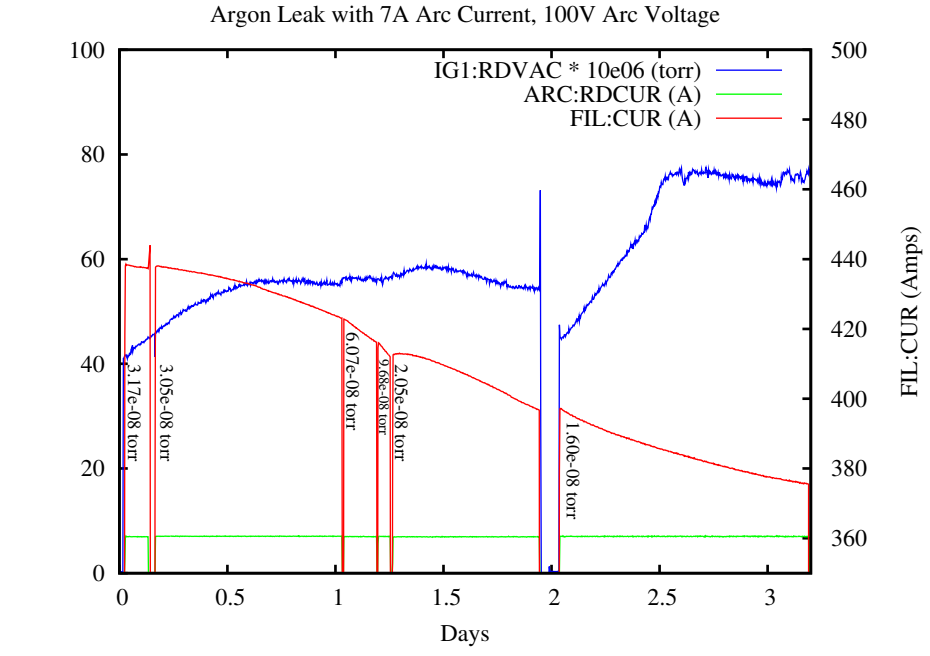

(b) Argon Leak

Figure 4: EPICS data from the series of neon and argon leaks. The variables are listed according to their names in EPICS: IG1:RDVAC is the vacuum pressure, ARC:RDCUR is the arc current, and FIL:CUR is the filament current. The scale on the left is for ARC:RDCUR and IG1:RDVAC×10e6, in the units listed in the legend. The start and end points of each leak is characterised by a sudden drop in filament current when the filament is turned off. The partial pressure of neon gas in the system during each leak is listed under the starting point of each leak curve. The EPICS data for the nitrogen and helium tests was not available at the time of writing.

3 I3 Pulser Electrode

3.1 Purpose

An electrode was installed in the I3 ion source with the ability to pulse the beam at low frequencies. The behaviour of the pulsed beam was studied to determine if the electrode was suitable for pulsing the beam at high frequencies.

3.2 Introduction

An H- ion source features a pair of electrodes: a plasma electrode, which shapes the plasma meniscus inside the source body, and an extraction electrode, which pulls H- ions out of the source to form a beam. These electrodes are disc-shaped with a small circular apertures at their center to allow beam current to be extracted through. Ion sources frequently have the ability to pulse the extracted beam. One method of pulsing a beam is to have an electrode near the extraction aperture, biased to prevent beam extraction, and have it rapidly switch on and off.

3.3 Equipment

The 1mm thick pulser electrode was installed between the two 1mm thick plasma electrodes with 1mm of spacing on either side. The aperture of the inner plasma electrode had a diameter of 5mm, the pulser electrode 7mm, and the outer plasma electrode 9mm. The extraction electrode was positioned . The extraction electrode was positively biased with respect to the source body while the plasma and pulser electrode were negatively biased. Pulsing was achieved by turning on and off the power supply to the pulser electrode with a controller. An electrometer was used to measure the beam current reaching a Faraday cup downstream of the source.

3.4 Method

Measurements were performed as follows:

- Source body voltage was set
- With the pulser electrode voltage at 0, beam current was maximized by adjusting the extraction and plasma electrode voltages
- Pulser electrode voltage was increased in steps and the minimum current was recorded at each step.

Tests were performed for source body voltages of 10kV, 15kV, and 20kV.

3.5 Results

Measurements from the tests are shown in Figure 4a. An electrostatic model of the ion source body was made in Opera and the potential along the axis was calculated for the configurations where beam cut-off was observed (Figure 4b). It is seen that a potential well of depth 120V is present near the pulser electrode when beam cut-off occurs (Since H- ions are negative this well acts as a barrier).

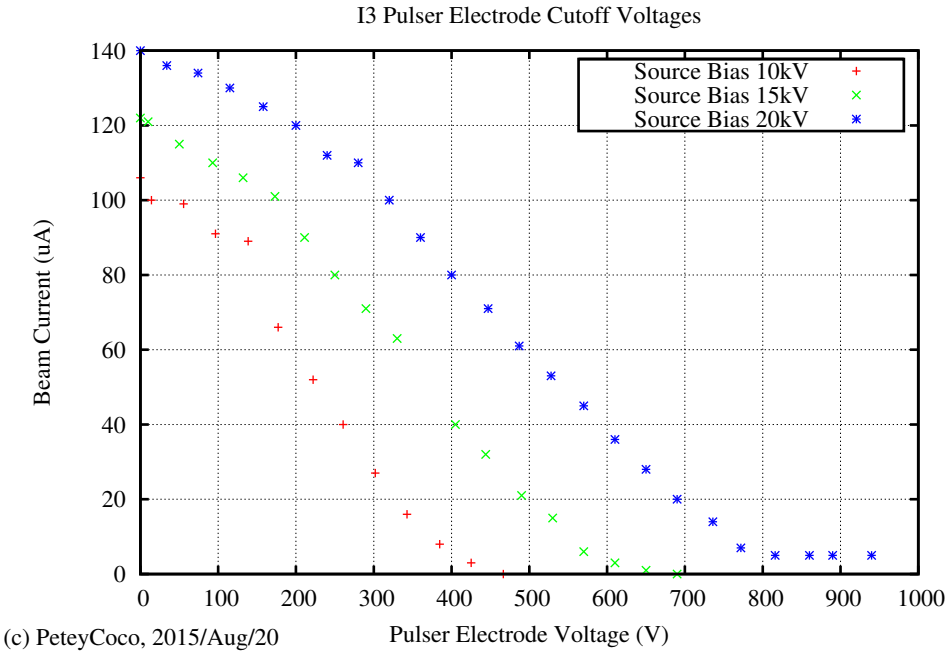

(a) Beam cut-off curves

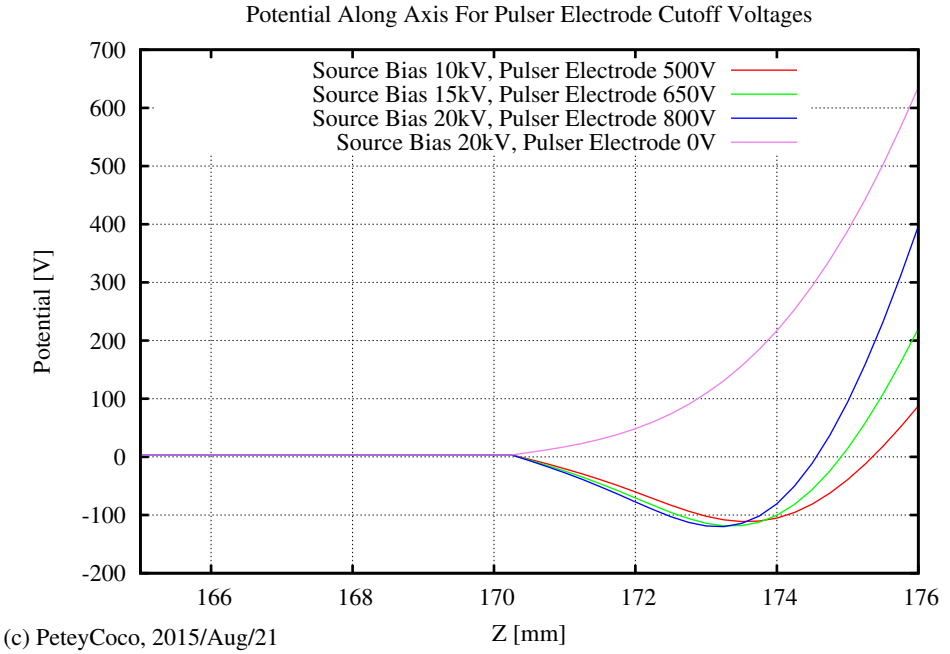

(b) Electrostatic model of source body

Figure 5: (a) Beam cut-off characteristic curve (b) The potential along the axis of the I3 ions source was calculated for the configurations where beam cut-off was observed. The potentials are plotted with the source body as ground. Z is measured from the backplate of the source body. The plasma electrode is located at 171mm and 175mm, the pulser electrode at 173mm, and the extraction electrode at 177 mm. It is seen that, for all source bias voltages, beam cut-off occurs when the potential forms a well with depth of approx. -120V.

3.6 Discussion

The existence of a potential well by the pulser electrode during cut-off suggests that the electrode method is not suitable for pulsing the beam at high frequencies. The plasma inside the source is slow to reach equilibrium, sometimes taking a few seconds to settle. With the current setup, the plasma meniscus is repeatedly being pulled out past the plasma electrode and pushed back into the source. At low frequencies this poses no issue, however as the frequency is increased the plasma meniscus will not have enough time to reach an equilibrium, leading to unpredictable beam performance.

4 Troubleshooting Beam Position in Injection Line

4.1 Introduction

The magnetic field inside the The purpose of this experiment was to determine the source of low-frequency, periodic disturbances in the beam's position along the injection line of the cyclotron.

4.2 Methods

A BPM measures the position of the beam in a plane perpendicular to its design trajectory. A pair of electrodes measure the position of the beam along a coordinate axis by the voltage induced on them when the beam, a current, deviates from the central position. Two such pairs of electrodes exist within the BPM to specify the horizontal and vertical position of the beam. The voltage signals from the electrodes are fed into an oscilloscope, where they can then be recorded and transferred to a computer for processing.

For this experiment, the signal from one set of electrodes on a BPM along the injection line was recorded and a Fourier analysis was performed on the data using a Python script.

4.3 Results

The results of the Fourier analysis are given in two plots: Figure 6a shows the entire frequency spectrum and Figure 6b shows the low-frequency harmonics. The amplitudes of the harmonics in both figures are normalized with respect to the largest harmonic.

4.4 Discussion

The 1.25Hz oscillation seen in Figure 6b corresponds to the original disturbance of interest. It was noticed while standing next to the injection line that the BPM signal on the oscilloscope "beats" in time with the sound of the vacuum pumps. A measurement of the pumping frequency of the vacuum pumps yielded 1.25Hz. Therefore the vacuum pumps on the injection line are likely the cause of low-frequency oscillations in the beam position.

Figure 6a reveals that higher-frequency disturbances exist that are not seen upon visual inspection of the BPM signal. The oscillations occurring at 60Hz, 119Hz, and 180Hz are attributable to poorly shielded electronic equipment along the beamline: Such equipment will produce stray electromagnetic fields that pulse at AC frequency, (i.e. 60Hz), as well as integer-multiples of this fundamental frequency, (e.g. 120Hz, 180Hz, and so on). The source of the oscillations in the neighbourhood of 22Hz has yet to be determined.

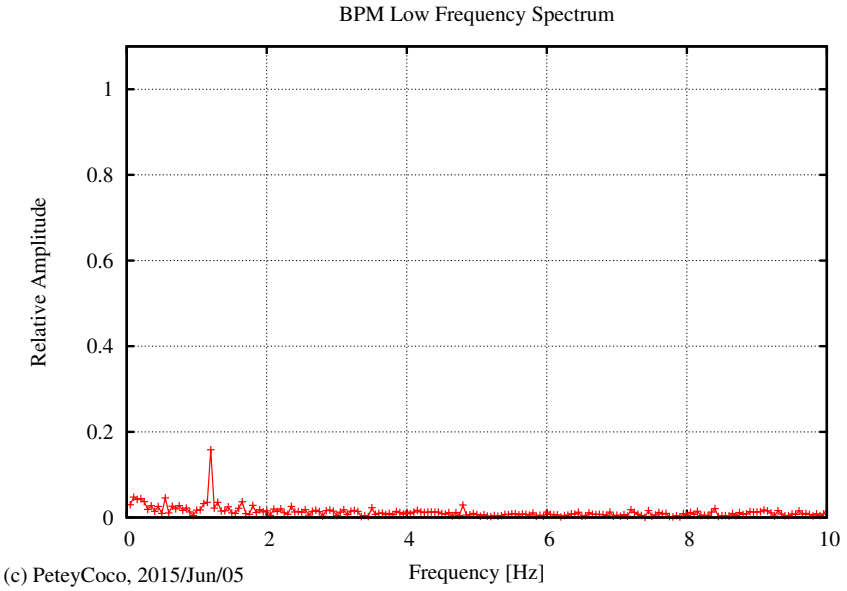

(a) Low Frequency Detail

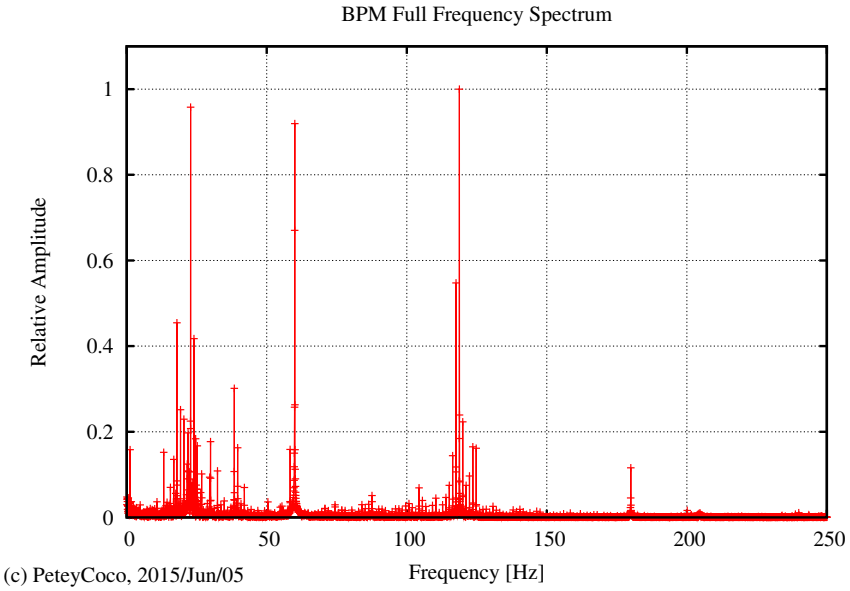

(b) Full Frequency Spectrum

Figure 6: Fourier analysis of BPM output. (a) Detailed view of low-frequency disturbances. Original disturbance of interest is seen to oscillate at 1.25Hz. (b) Plot of the entire frequency spectrum. The largest disturbances occur at 22Hz, 60Hz, and 119Hz.

Bibliography

[1] Chao, A. (2013). Magnetic Measurements. In M. Tigner (Ed.), Handbook of Accelerator Physics and Engineering (Second ed.). World Scientific Publishing Company.

[2] Schmidt, Charles W. (1990, September). Review of Negative Hydrogen Ion Sources. Paper presented at Linear Accelerator Conference, Albuquerque, New Mexico. Place of Publication: Los Alamos National Laboratory, 1991